Linear Cationic Click Polymer for Gene Delivery: Synthesis, Biocompatibility, and In Vitro Transfection

Yu Gao, Lingli Chen, Zhiwen Zhang, Wangwen Gu, and Yaping Li*

Center of Pharmaceutics, Shanghai Institute of Materia Medica, Chinese Academy of Sciences, Shanghai 201203, China

Received August 5, 2010; Revised Manuscript Received September 7, 2010

Sixteen novel cationic click polymers (CPs) were parallelly synthesized via the conjugation of four alkyne-functionalized monomers to four azide-functionalized monomers by "click chemistry". The biocompatibility of CPs was evaluated by in vitro cytotoxicity (MTT assay, Hoechst/PI apoptosis/necrosis assay, and cell cycle analysis) and blood compatibility tests (hemolysis and erythrocyte aggregation). The experimental results showed that the kind of amine groups, charge density, and number of methylene or ethylene glycol groups brought about the effect on toxicity of CPs. Among all polymers, two polymers ($\mathbf{B_1}$ and $\mathbf{B_2}$) showed good biocompatibility, inducing neither apoptosis nor necrosis at the test concentration and low hemolysis ratio and erythrocyte aggregation. In particular, $\mathbf{B_1}$ and $\mathbf{B_2}$ exhibited the comparable transfection efficiency compared with PEI (25 kDa) but much lower cytotoxicity. These results suggested that the novel cationic CPs could be promising carriers for gene delivery.

1. Introduction

Cationic polymers have attracted the great interest and attention as nonviral gene vectors because of their merits in avoidance of potential immunogenicity, large gene loading capacity, and the ease of large-scale preparation.[1,2] The cationic polymers could electrostatically interact with negatively charged DNA or RNA and condense them into polyplexes, which could enter cells via endocytosis. However, the current several important cationic polymers for gene delivery are not fully effective in vivo because of their toxicity or the instability of polyplexes in serum.[3−5] Therefore, it is still challenging work to design rationally the new cationic polymers with defined molecular structure that are biocompatible and applicable for more efficient gene delivery.

In recent years, the concept of click chemistry, introduced by Sharpless et al.,[28] has been regarded as a powerful tool in the design and synthesis of materials. The copper-catalyzed azide−alkyne cycloaddition (CuAAC), which is a unique ligation method combining selective reactivity and easy manufacturing, is generally regarded as the quintessential example of click chemistry,[6,7] which has rapidly found utilization in numerous fields including in a variety of polymer syntheses such as the block copolymers,[8] dendrimers,[9,10] graft copolymers,[11] and adhesive polymers.[12] In the linear polymer synthesis, the azide- or alkyne-functionalized monomers could be easily tailored to form the different copolymers with different chemical and biological properties.[13] The unique 1,2,3-triazole-amide moiety, which was formed during polymerization, could be H-bond acceptors and increase hydrophobic interactions of the polymer with DNA.[14] This characteristics makes the linear cationic click polymer (CP) bind effectively with DNA to improve stability of polyplexes. Although the linear cationic CP demonstrated the great potential for gene delivery, the syntheses and applications of cationic CP for gene delivery are still very few,[14,15] and the structure−biocompatibility relationship of the linear CP has not been investigated until today.

Parallel synthesis has gained increasing popularity as a means to synthesize the diverse polymer libraries with different chemical or biological properties.[16,17] Screening of the library of polymers could rapidly identify the novel polymers for gene delivery with the high transfection efficiency and low cytotoxicity.[16−19] We are interested in developing a library of novel linear cationic CPs with good biocompatibility for gene delivery. In this work, 16 cationic CPs were parallelly synthesized via the conjugation of four alkyne-functionalized monomers to four azide-functionalized monomers by "click chemistry", and the biocompatibility of CPs was evaluated by in vitro cytotoxicity and blood compatibility. Finally, the in vitro transfection efficiency of two CPs with good biocompatibility was evaluated in MDA-MB-468 cells.

2. Experimental Section

2.1. Materials. Diethylenetriamine, triethylenetetramine, diethylene glycol, triethylene glycol, diethanolamine, *N*-methyldiethanolamine, di-*tert*-butyl dicarbonate, 4-dimethylamino pyridine (DMAP), copper(II) sulfate, sodium azide, trifluoroacetic acid, and *p*-toluenesulfonyl chloride (TsCl) were obtained from Sinopharm Group Chemical Reagent (China). *N*-(*tert*-Butoxycarbonyl)-L-aspartic acid, *N*,*N*′-dicyclohexylcarbodiimide (DCC), 1-ethyl-3-(3-dimethyllaminopropyl)carbodiimide hydrochloride (EDC·HCl), and *N*-(*tert*-butoxycarbonyl)-L-glutamic acid were purchased from GL Biochem (Shanghai, China). Trypsin-EDTA and phosphate-buffered saline (PBS) were obtained from Gibco-BRL (Burlington, ON, Canada). The RPMI 1640 medium, antibiotics, and fetal bovine serum (FBS) were purchased from Invitrogen GmbH (Karlsruhe, Germany). Branched polyethylenimine (PEI, 25 kDa), 3-(4,5-dimethylthiazol-2-yl)-2,5-diphenyltetrazolium bromide (MTT), DNA-free RNase A, Hochest 33342, propidium iodide (PI), propiolic acid, propargylamine, and ethyl trifluoroacetate were purchased from Sigma (St. Louis, MO). All other chemicals and solvents, if not mentioned, were of analytical grade and used as received without additional purification.

Plasmid EGFP-N1 (4.7 kb) encoding enhanced green fluorescent protein driven by immediate early promoter of CMV was purchased

* To whom correspondence should be addressed. Address: 501 Haike Road, Shanghai 201203, China. Phone: +86-21-2023-1979. Fax: +86-21-2023-1979. E-mail: ypli@mail.shcnc.ac.cn.

10.1021/bm100906m © 2010 American Chemical Society
Published on Web 09/28/2010

Scheme 1. Synthetic Routes for Monomers

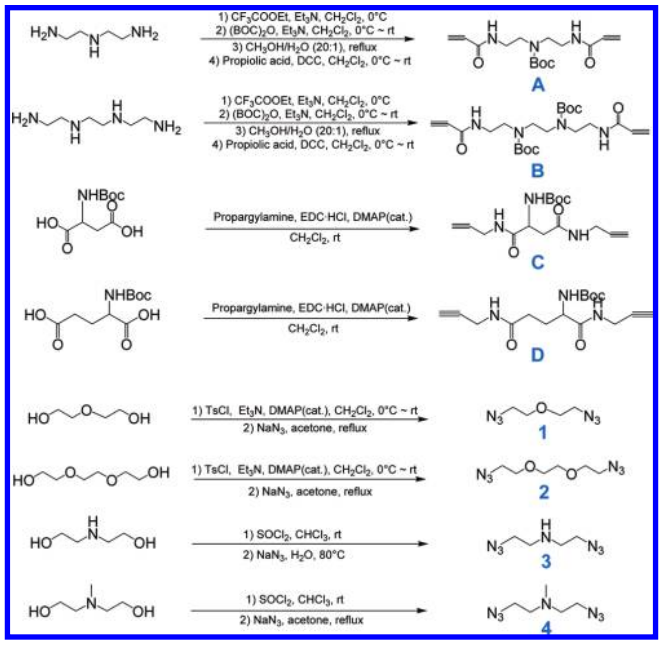

from Clontech (Palo Alto, CA). The plasmid DNA (pDNA) grown in DH5α strain of *E. coli* was isolated with the EndFree Plasmid Mega Kit (Qiagen GmbH, Hilden, Germany). The purity was confirmed by spectrophotometry (A260/A280), and DNA concentration was measured by UV absorption at 260 nm.

2.2. Cell Culture. The cell line MDA-MB-468 (human breast cancer cell) was obtained from the American Type Culture Collection (ATCC, Manassas, VA). MDA-MB-468 cells were cultured in RPMI 1640 medium supplemented with 10% FBS and 1% antibiotics (100 U/mL penicillin G and 0.1 mg/mL streptomycin). Cells were maintained at 37 °C in a humidified and 5% CO_2 incubator.

2.3. Synthesis of Monomers. *2.3.1. General.* The synthetic routes for monomers were shown in Scheme 1. TLC was performed on silica gel and detected by UV light, $KMnO_4$, and I_2 wherever applicable. The ^{1}H spectra were recorded on a Bruker 400 MHz NMR spectrometer. The ^{1}H NMR spectrum was as follows: chemical shift (δ), multiplicity (s = singlet, d = doublet, t = triplet, m = multiplet, dd = double doublets, bs = broad singlet, bm = broad multiplet), J coupling constant (hertz), and the peak integration. Gel permeation chromatography (GPC) was conducted on a Waters 2695 controller equipped with an ULTRAHYDROGEL column 250 PKGD and a refractive index detector (model 2414) for the estimation of the molecular weight of CPs. The mobile phase is the water-containing sodium azide (0.05%, w/v) at a flow rate of 0.5 mL/min with a column temperature of 30 °C. The polymer was dissolved in water (0.05% sodium azide), and the sample was analyzed and calibrated by DEXTRAN standards (Mp = 4400−401 000 Da, American Polymer Standards Corporation).

*2.3.2. Bis-(2-propynoylamino-ethyl)-carbamic Acid tert-Butyl Ester (**A**).* Bis-(2-propynoylamino-ethyl)-carbamic acid *tert*-butyl ester was obtained using a four-step synthesis procedure, as previously reported with minor modification.[14] In brief, ethyl trifluoroacetate (2.95 g, 21 mmol) was added dropwise to diethylenetriamine (1.03 g, 10 mmol) dissolved in dichloromethane (50 mL) at 0 °C. After being stirred for 1 h at room temperature, a solution of di-*tert*-butyl dicarbonate (3.28 g, 15 mmol) in dichloromethane and triethylamine (1.52 g, 15 mmol) were added dropwise to this mixture. The solution was stirred overnight and then washed with aqueous $NaHCO_3$. The organic layer was separated, dried over Na_2SO_4, and evaporated. The crude product was purified by recrystallization from CH_2Cl_2/hexane. The yielding protected oligoamine (2.00 g) was then refluxed in methanol/water (volume ratio, 20:1, containing 1.80 g K_2CO_3) for 4 h. After the methanol was evaporated, the residue was extracted with dichloromethane. The organic layers were combined, dried over Na_2SO_4, and evaporated to yield the compound bis-(2-amino-ethyl)-carbamic acid *tert*-butyl ester as a waxy solid.

Propiolic acid (0.38 g, 5.4 mmol) was added to a solution of DCC (1.25 g, 6 mmol) in dichloromethane (100 mL) at 0 °C under N_2 and stirred for 2 h. A solution of bis-(2-amino-ethyl)-carbamic acid *tert*-butyl ester (0.50 g, 2.4 mmol) dissolved in dichloromethane was then added dropwise to this mixture, and the reaction mixture was stirred for 2 h at 0 °C. The mixture was then warmed to room temperature and stirred for an additional 24 h. After the white solid was filtered, the solvent was evaporated, and the resulting crude product was purified via silica gel chromatography using a gradient elution of 2 to 4% methanol in chloroform (Rf = 0.3 for **A** in 4% MeOH/$CHCl_3$) to yield the final product as pale yellow solid. ^{1}H NMR ($CDCl_3$): 6.86 (bs, 2H), 3.49−3.41 (m, 8H), 2.82 (s, 2H), 1.49 (s, 9H).

*2.3.3. {2-[tert-Butoxycarbonyl-(2-propynoylamino-ethyl)-amino]-ethyl}-(2-propynoylamino-ethyl)-carbamic Acid tert-Butyl Ester (**B**).* Compound **B** was prepared using a four-step synthesis procedure with triethylenetetramine as the starting material in a similar manner as diethylenetriamine. Compound **B** was obtained as pale yellow solid. ^{1}H NMR ($CDCl_3$): 8.14 (bs, 2H), 3.22−3.48 (m, 8H), 2.75 (s, 2H), 1.49 (s, 18H).

*2.3.4. (1,2-Bis-prop-2-ynylcarbamoyl-ethyl)-carbamic Acid tert-Butyl Ester (**C**).* To a stirred solution of (1,2-dicarbamoyl-ethyl)-carbamic acid *tert*-butyl ester (2.33 g, 10 mmol) in dichloromethane (100 mL), EDC·HCl (4.34 g, 22 mmol) and DMAP (0.24 g, 2 mmol) were added and stirred for 2 h. To this mixture, a solution of propargylamine (1.21 g, 22 mmol) dissolved in 25 mL of dichloromethane was added at 0−10 °C. Then, the reaction mixture was stirred under N_2 for 24 h at room temperature. After the solvent evaporated, the resulting crude product was purified via silica gel chromatography using a gradient elution of 2 to 4% methanol in chloroform (Rf = 0.3 for **C** in 4% MeOH/$CHCl_3$). The proper fractions were combined, the solvent was evaporated, and the resulting white solid was isolated. ^{1}H NMR ($CDCl_3$): 7.15 (bs, 1H), 6.26 (bs, 1H), 6.11 (m, 1H), 4.46 (m, 1H), 3.93−3.10 (m, 4H), 2.88 (dd, J = 3.9 Hz, 4H), 2.55 (dd, J = 6.4 Hz, 1H), 2.52−2.59 (m, 1H), 2.22−2.23 (m, 1H), 1.45 (s, 9H).

*2.3.5. (1,3-Bis-prop-2-ynylcarbamoyl-propyl)-carbamic Acid tert-Butyl Ester (**D**).* To a stirred solution of (1,3-dicarbamoyl-propyl)-carbamic acid *tert*-butyl ester (2.47 g, 10 mmol) in dichloromethane (100 mL), EDC·HCl (4.34 g, 22 mmol), and DMAP (0.24 g, 2 mmol) were added and stirred for 2 h. To this mixture, a solution of propargylamine (1.21 g, 22 mmol) dissolved in 25 mL of dichloromethane was added at 0−10 °C. The reaction mixture was then stirred under N_2 for 24 h at room temperature. After the solvent evaporated, the resulting crude product was purified via silica gel chromatography using a gradient elution of 2 to 4% methanol in chloroform (Rf = 0.3 for **D** in 4% MeOH/$CHCl_3$). The proper fractions were combined, the solvent was evaporated, and the resulting white solid was isolated. ^{1}H NMR ($CDCl_3$): 7.21 (bs, 1H), 6.58 (bs, 1H), 5.73 (d, J = 7.5 Hz), 4.17−4.19 (m, 1H), 4.02−4.06 (m, 4H), 2.32−2.40 (m, 2H), 2.21−2.25 (m, 2H), 1.96−2.11 (m, 2H), 1.46 (s, 9H).

*2.3.6. 1-Azido-2-(2-azido-ethoxy)-ethane (**1**).* To a stirred solution of diethylene glycol (2.12 g, 20 mmol) in dichloromethane (250 mL) at 0 °C, triethylamine (4.25 g, 42 mmol), DMAP (0.12 g, 0.1 mmol), and TsCl (7.62 g, 42 mmol) were added. The mixture was stirred at 0−10 °C for 1 h, then at room temperature for 12 h. The reaction solution was extracted with saturated $NaHCO_3$ solution (2 × 300 mL) and then with saturated NaCl solution (300 mL). The organic layers were dried over Na_2SO_4, and the dichloromethane was evaporated to yield the off-white solid. The crude product was purified by recrystallization from CH_2Cl_2/petroleum ether to yield white solid 2,2′-oxybis(ethane-2,1-diyl) bis(4-methylbenzenesulfonate).

To a solution of 2,2′-oxybis(ethane-2,1-diyl) bis(4-methylbenzenesulfonate) (4.1 g, 10 mmol) in acetone, sodium azide (1.9 g, 30 mmol) was added, and the mixture was refluxed for 48 h. After the solvent was evaporated, the resulting crude product was purified via silica gel

Scheme 2. Synthetic Routes for Polymers

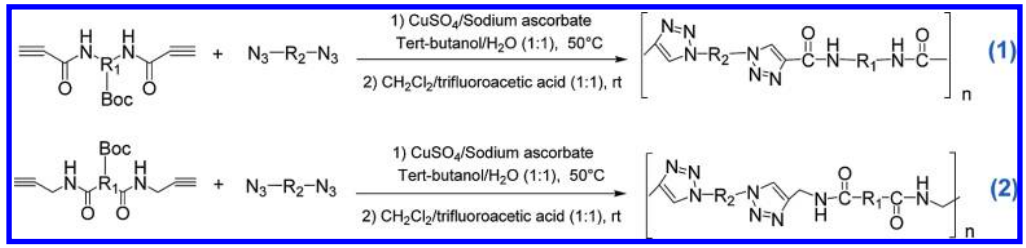

chromatography using an elution of 50% ethyl acetate in petroleum ether (Rf = 0.8 for **1** in 50% ethyl acetate/petroleum ether). The proper fractions were combined, and the solvent was evaporated to yield **1** as yellow oil. ^{1}H NMR ($CDCl_3$): 2.87 (s, 4H), 2.70 (s, 4H).

*2.3.7. 1-Azido-2-[2-(2-azido-ethoxy)-ethoxy]-ethane (**2**).* To a stirred solution of triethylene glycol (3.00 g, 20 mmol) in dichloromethane (250 mL) at 0 °C, triethylamine (4.25 g, 42 mmol), DMAP (0.12 g, 0.1 mmol), and TsCl (7.62 g, 42 mmol) were added. The mixture was stirred at 0−10 °C for 1 h, then at room temperature for 12 h. The reaction solution was extracted with saturated $NaHCO_3$ solution (2 × 300 mL), then with saturated NaCl solution (300 mL). The organic layers were dried over Na_2SO_4, and the dichloromethane was evaporated to yield the off-white solid. The crude product was purified by recrystallization from CH_2Cl_2/petroleum ether to yield white solid 2,2′-(ethane-1,2-diylbis(oxy))bis(ethane-2,1-diyl) bis(4-methylbenzenesulfonate).

To a solution of 2,2′-(ethane-1,2-diylbis(oxy))bis(ethane-2,1-diyl) bis(4-methyl -benzenesulfonate) (4.6 g, 10 mmol) in acetone, sodium azide (1.9 g, 30 mmol) was added, and the mixture was refluxed for 48 h. After the solvent was evaporated, the resulting crude product was purified via silica gel chromatography using an elution of 50% ethyl acetate in petroleum ether (Rf = 0.8 for **2** in 50% ethyl acetate/petroleum ether). The proper fractions were combined, and the solvent was evaporated to yield **2** as yellow oil. ^{1}H NMR ($CDCl_3$): 3.65−3.69 (m, 8H), 3.37 (t, J = 5.2 Hz, 4H).

*2.3.8. Bis-(2-azido-ethyl)-amine (**3**).* To a solution of diethanolamine (7.7 g, 100 mmol) in chloroform (100 mL) at 0 °C, thionyl chloride (47.6 g, 400 mmol) dissolved in chloroform (20 mL) was added dropwise for 1 h. The solution was then stirred for 24 h at room temperature. The solvent was evaporated, and the crude product was purified by recrystallization from $CHCl_3$/petroleum ether to yield the bis-(2-chloro-ethyl)-amine hydrochloride as a white solid.

A solution of bis-(2-chloro-ethyl)-amine hydrochloride (1.8 g, 10 mmol) and sodium azide (3.3 g, 50 mmol) in water (50 mL) was heated at 80 °C for 24 h. After evaporating most of the water, the solution was made basic with sodium hydroxide and then extracted with diethyl ether. The organic phase was combined and dried over potassium carbonate. After evaporating the solvent, the resulting crude product was purified via silica gel chromatography using an elution of 50% ethyl acetate in petroleum ether (Rf = 0.5 for **3** in 50% ethyl acetate/petroleum ether). The proper fractions were combined, and the solvent was evaporated to yield **3** as yellow oil. ^{1}H NMR ($CDCl_3$): 3.40 (t, J = 5.4 Hz, 4H), 2.79 (t, J = 4.8 Hz, 4H).

*2.3.9. Bis-(2-azido-ethyl)-methyl-amine (**4**).* To a solution of *N*-methyldiethanolamine (11.9 g, 100 mmol) in chloroform (100 mL) at 0 °C, thionyl chloride (47.6 g, 400 mmol) dissolved in chloroform (20 mL) was added dropwise for 1 h. The solution was then stirred for 24 h at room temperature. The solvent was evaporated, and the crude product was purified by recrystallization from $CHCl_3$/petroleum ether to yield the bis-(2-chloro-ethyl)-methyl-amine hydrochloride as white solid.

The obtained bis-(2-chloro-ethyl)-methyl-amine hydrochloride was dissolved in saturated solution of $NaHCO_3$, and the solution was then extracted with dichloromethane. The organic layers were dried over Na_2SO_4, and the dichloromethane was evaporated to yield the bis-(2-chloro-ethyl)-methyl-amine as a yellow oil.

To a solution of bis-(2-chloro-ethyl)-methyl-amine (1.6 g, 10 mmol) in acetone, sodium azide (3.3 g, 50 mmol) was added, and the mixture was refluxed for 48 h. After the solvent evaporated, the resulting crude product was purified via silica gel chromatography using an elution of 50% ethyl acetate in petroleum ether (Rf = 0.5 for **4** in 50% ethyl acetate/petroleum ether). The proper fractions were combined, and the solvent was evaporated to yield **4** as yellow oil. ^{1}H NMR ($CDCl_3$): 3.33 (t, J = 6.0 Hz, 4H), 2.63 (t, J = 6.0 Hz, 4H), 2.32 (s, 3H).

2.4. Synthesis of CPs. The synthetic routes for CPs were shown in Scheme 2. For synthesis of CP $\mathbf{A_1}$, the solution of copper(II) sulfate (0.032 g, 0.2 mmol) in water (0.5 mL) was added to the solution of monomer **A** (0.31 g, 1 mmol) and monomer **1** (0.16 g, 1 mmol) dissolved in *tert*-butanol (1 mL), and the mixture was introduced to a small vial covered with a rubber cap. The vial was filled with nitrogen in vacuum. The solution of sodium ascorbate (0.079 g, 0.4 mmol) dissolved in 0.5 mL of water was added dropwise with a thin pinhead piercing through the rubber cap. The mixture was heated to 50 °C in an oil bath, stirred for 24 h. The solvents were evaporated, and the resulting copolymer was then dissolved in 10 mL of a solution of dichloromethane/trifluoroacetic acid (1:1 volume) with stirring for 3 h and dried under vacuum. The final product after neutralization using 1 M NaOH solution was purified via dialysis against 0.01 M HCl for 24 h, then exhaustively against ultra pure H_2O for 3 days. The final deprotected polymers were lyophilized to yield a brown solid. ^{1}H NMR (D_2O): 7.94 (s, 2H), 4.34−4.29 (m, 4H), 3.70 (bs, 4H), 3.39−3.45 (m, 4H), 2.75−2.87 (m, 4H).

The other CPs were prepared from alkyne-functionalized monomers and azide-functionalized monomers using a similar method as $\mathbf{A_1}$ and analyzed by ^{1}H NMR (D_2O). The data are listed as below: $\mathbf{A_2}$: ^{1}H NMR (D_2O): 8.05 (s, 2H), 4.50 (bs, 4H), 3.82 (bs, 4H), 3.61 (bs, 8H), 3.20 (bs, 4H). $\mathbf{A_3}$: ^{1}H NMR (D_2O): 8.59 (bs, 2H), 3.84−3.71 (m, 8H), 3.48 (m, 8H). $\mathbf{A_4}$: ^{1}H NMR (D_2O): 8.00−8.02 (m, 2H), 4.35−4.62 (m, 4H), 3.65−3.70 (m, 4H), 3.39−3.53 (m, 4H), 2.84−2.92 (m, 4H), 2.35 (s, 3H). $\mathbf{B_1}$: ^{1}H NMR (D_2O): 8.07 (s, 2H), 4.53 (bs, 4H), 3.91 (bs, 4H), 3.61 (bs, 4H), 2.17−3.22 (m, 8H). $\mathbf{B_2}$: ^{1}H NMR (D_2O): 8.23 (s, 2H), 4.54−4.60 (m, 4H), 3.88 (s, 4H), 3.53−3.63 (m, 8H), 3.14−3.20 (m, 8H). $\mathbf{B_3}$: ^{1}H NMR (D_2O): 8.60 (bs, 2H), 3.83−3.86 (m, 8H), 3.41−3.59 (m, 12H). $\mathbf{B_4}$: ^{1}H NMR (D_2O): 8.10−8.18 (m, 2H), 4.43 (bs, 4H), 3.70−3.73 (m, 4H), 3.26−3.32 (m, 8H), 2.96−2.98 (m, 4H), 2.37 (s, 3H). $\mathbf{C_1}$: ^{1}H NMR (D_2O): 7.52 (s, 2H), 4.20−4.30 (m, 8H), 3.63−3.67 (m, 5H), 3.70 (bs, 2H). $\mathbf{C_2}$: ^{1}H NMR (D_2O): 7.83−7.84 (m, 2H), 4.47−4.48 (m, 4H), 4.40−4.42 (m, 2H), 4.35 (bs, 2H), 3.80−3.82 (m, 5H), 3.51 (bs, 4H), 2.84−2.86 (m, 2H). $\mathbf{C_3}$: ^{1}H NMR (D_2O): 7.94 (bs, 2H), 4.63−4.73 (m, 4H), 4.56−4.59 (m, 4H), 3.29−3.39 (bs, 5H), 2.96 (bs, 2H). $\mathbf{C_4}$: ^{1}H NMR (D_2O): 7.85−7.92 (m, 2H), 4.52−4.72 (m, 8H), 2.82−3.15 (m, 5H), 2.25−2.46 (m, 5H). $\mathbf{D_1}$: ^{1}H NMR (D_2O): 7.81 (s, 2H), 4.45−4.52 (m, 8H), 3.89 (bs, 4H), 3.79 (bs, 1H), 2.45 (bs,2H), 2.19 (bs, 2H). $\mathbf{D_2}$: ^{1}H NMR (D_2O): 7.91−7.92 (m, 2H), 4.44−4.55 (m, 8H), 3.87 (bs, 4H), 3.52−3.66 (m, 5H), 2.32 (t, J = 3.6 Hz, 2H), 1.95 (bs, 2H). $\mathbf{D_3}$: ^{1}H NMR (D_2O): 7.85−7.89 (m, 2H), 4.32−4.45 (m, 8H), 3.92 (bs, 1H), 3.08 (bs, 4H), 2.35−2.37 (m, 2H), 2.09 (bs, 2H). $\mathbf{D_4}$: ^{1}H NMR (D_2O): 7.91 (s, 2H), 4.43−4.56 (m, 8H), 4.09 (bs, 1H), 3.16 (bs, 4H), 2.48 (bs, 5H), 2.20 (bs, 2H).

2.5. MTT Assay. MDA-MB-468 cells were seeded at a density of 1×10^4 cells per well in 150 μL of growth medium in 96-well plates and grown overnight. Immediately after growth medium was removed,

CPs were applied to the cells in fresh culture media with 10% FBS at polymer concentrations from 5 to 200 μg/mL. Cells treated with fresh culture media only were used as control. After 24 h of incubation, the polymer-containing media were replaced with fresh culture media containing MTT solution (0.2 mg/mL), and the cells were incubated for an additional 4 h at 37 °C. Then, the medium was removed, and DMSO was added to dissolve the crystal. The plates were mildly shaken for 10 min to ensure the dissolution of formazan. The absorbency values were measured by TECAN Infinite F200 multimode microplate reader (Salzburg, Austria) at wavelength 570 nm, blanked with DMSO solution. Six replicates were counted for each sample.

2.6. Apoptosis or Necrosis Observation. The apoptosis or necrosis was detected by assessment of nuclear double-staining with Hoechst 33342 and PI. In brief, $\sim 1 \times 10^6$ MDA-MB-468 cells treated with 100 μg/mL CPs for 24 h were collected by centrifugation, washed twice with PBS (pH 7.4), and resuspended in 250 mL of PBS (pH 7.4) containing 10 μg/mL Hoechst 33342 and 20 μg/mL PI in dark at room temperature for 15 min and then observed with a fluorescence microscope (E800, Nikon) and documented by photography.

2.7. Cell Cycle Analysis. Cell cycle analysis was assessed by flow cytometry.[20] In brief, cells seeded on the six-well plate were treated with 100 μg/mL CPs for 24 h. Cells (1×10^6) were collected, washed twice with PBS, and then fixed with 70% precooled ethanol and stored at 4 °C for 24 h. Cells were centrifugated, washed with cold-PBS twice and incubated with RNase A (10 mg/mL) for 20 min at 37 °C, and stained with PI (2 mg/mL) for 30 min in the dark. The DNA content was measured by FACSCalibur system (Becton Dickinson). The percentage of DNA at G0/G1, S, and G2/M phases of the cell cycle could be determined from the flow histograms, and apoptotic cells with degraded DNA appeared in the area left to the G0/G1 peak, which was the so-called "SubG1" phase on the DNA histogram.

2.8. Hemolysis Assay. Fresh blood from ICR rats was collected in heparinized tubes. Erythrocytes were washed three times and suspended in 0.9% NaCl solution (2% (v/v)). Washed erythrocytes were incubated with CPs at polymer concentration of 100 μg/mL, 0.9% NaCl solution (negative control group with 0% hemolysis), or DD water (positive control group with 100% hemolysis) for 3 h at 37 °C. After centrifugation at 1000 rpm for 5 min, the absorbance of the supernatant was determined at 540 nm. The percent of hemolysis was calculated by $(T_i - T_0)/(T_{max} - T_0) \times 100\%$, where T_i was the average absorbance of the CP-treated group, T_0 was the average absorbance of the negative control group, and T_{max} was the average absorbance of the positive control group.

2.9. Erythrocyte Aggregation Assay. The washed erythrocyte suspension was mixed with polymer solution to get a final polymer concentration 100 μg/mL and incubated for 3 h at 37 °C. Aggregation of erythrocytes was evaluated under an optical microscope.

2.10. In Vitro Transfection. For in vitro transfection, CP/DNA complex nanoparticles (CPNs) were prepared. In brief, pDNA (100 μg/mL) dissolved in sterile water was added to the CP solution diluted in sterile water with equal volume to obtain the desired polymer-amine to DNA-phosphate ratio (N/P ratio). Subsequently, solution was immediately vortexed for 30 s (XW-80A Votex mixer, Shanghai). The resulting CPNs were allowed to sit at room temperature for 30 min. As positive control, PEI 25K/DNA complex nanoparticles (PEINs) were prepared with the same procedure as CPNs. The particle size and ζ potential of CPNs were determined by the laser light scattering measurement using a Nicomp 380/ZLS zeta potential analyzer (Particle Sizing System).

MDA-MB-468 cells were seeded in 24-well plates at a density of 1×10^5 cells per well in 500 μL of complete medium and incubated for 24 h prior to transfection. Then, the media were replaced with fresh complete growth medium containing CPNs with DNA concentration 2.5 μg/well at various N/P ratios. Media were replaced by fresh culture medium after 24 h, and cells were incubated for an additional 24 h. The expressed green protein could be observed under a fluorescence microscope. Finally, cells were collected and resuspended in PBS (pH 7.4). The transfection results were measured using a FACSCalibur through FL1. As control, naked DNA was used on cell cultures and examined as described above. As positive control, PEINs with mass ratio 3 were prepared and transfected with media without FBS for 2 h before the medium was replaced with fresh complete growth medium.

3. Results and Discussion

3.1. Monomer Choosing and Polymer Synthesis. Alkyne-functionalized monomers **A**−**D** and azide-functionalized monomers **1**−**4** representing either structural or functional character were selected for the synthesis of the CPs. Changing azide-functionalized monomers while keeping the alkyne-functionalized monomer unaltered, the differences between polymers could be measured, the different functions of the groups on the azide-functionalized monomers could be deduced, and vice versa. All polymers were designed to be water-soluble and had aliphatic amines that were able to interact electrostatically with plasmid DNA. Monomers containing aromatic amines were not chosen for polymer synthesis because of the decreased alkalinity of the amine and the hydrophobicity of the aromatic ring. Because the types of amino groups and charge density have been considered to be one of the most important factors influencing the property of cationic gene vectors,[14,21,22] the monomers were chosen with different types of amino groups and different distance between charge groups. Comparing **A** with **C** or **3** with **4**, the different functions of the primary, secondary, or the tertiary amine on the CP backbone could be found. Comparing **A** with **B**, the influence of charge density on the property of CP could be found. The monomers were also designed with a different number of ethylene glycol or methylene groups because the previous reports demonstrated that the degree of hydrophobicity and hydrophilicity of polymer played an important role in affecting the polymer function,[23−26] and the number of methylene on the polymer side chains showed the great effects on the transfection efficiency and cytotoxicity of polymers.[27] The function of the ethylene glycol group could be found by comparing **1** or **2** containing ethylene glycol with other azide-functionalized monomers, and the effect of the number of ethylene glycol on polymer properties could be found by comparing **1** with **2**. The role of the methylene on the backbone of CP could be investigated by comparing **C** with **D**, between which there was one methylene variation.

Polymers were synthesized with alkyne-functionalized monomers and azide-functionalized monomers in equal molar ratios via "click polymerization" by a similar method exploited by Sharpless et al.[28,29] Solution of *tert*-butyl alcohol and water (1:1, v/v) was chosen as a general solvent for polymer synthesis on the basis of solubility of all monomers. Copper(II) sulfate pentahydrate and sodium ascorbate were chosen as catalysts, and polymerization proceeded at 50 °C with similar monomer concentration to yield polymers with the similar degree of polymerization. To yield the final polymers, the Boc groups on the alkyne-functionalized monomers were deprotected with trifluoroacetic acid in dichloromethane. The final 16 products (4 alkynes × 4 azides = 16 polymers) were all water-soluble, and the Boc protecting groups were completely cleaved from the polymer backbone according to ^{1}H NMR analysis. The representative ^{1}H NMR spectra of polymer $\mathbf{B_1}$ and $\mathbf{B_2}$ were shown in Figure 1. The signals δ at ~8 were assigned to the triazole groups. The relative weight molecular weights of CPs ranged from (1.2 to 1.8) $\times 10^4$ measured by GPC. All polymers were successfully synthesized with similar degrees of polym-

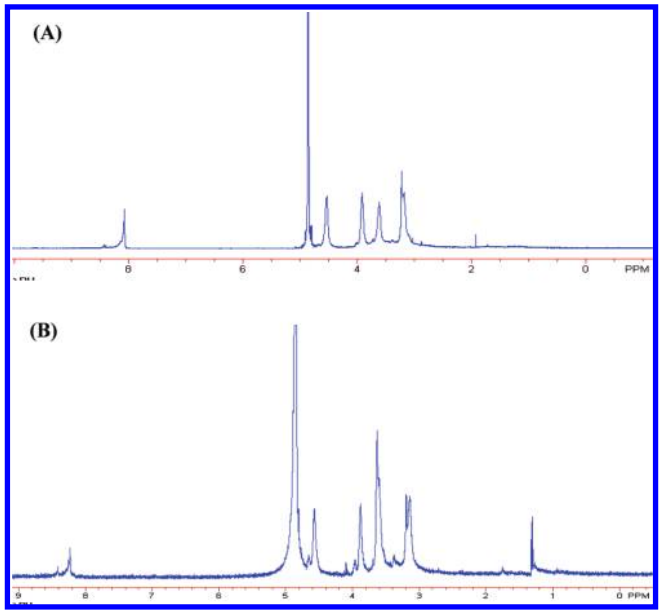

Figure 1. ^{1}H NMR spectra of polymer (A) $\mathbf{B_1}$ and (B) $\mathbf{B_2}$.

erization to elucidate the effect of different functional groups on polymer backbone on biocompatibility of polymers (Table 2).

3.2. MTT Assay. Among all methods utilized for the biocompatibility study, the in vitro experiment with the cultured cell line is the most common. The cytotoxicity of CPs was detected on MDA-MB-468 cell lines by MTT assay. Relative to the polymers $\mathbf{C_2}$, $\mathbf{A_3}$, $\mathbf{A_4}$, $\mathbf{B_3}$, and $\mathbf{B_4}$, the other 11 polymers showed low cytotoxicity in MDA-MB-468 cells with cell viability of ~75% at 100 μg/mL polymer (Figure 2). The toxicity of CPs increased with polymer concentration increasing. In the cell viability curves, it was very obvious that **C** and **D** series showed much lower cytotoxicity than **A** or **B** series, which indicated that polymers synthesized using alkyne-functionalized monomers with secondary amine were much more toxic than polymers synthesized using alkyne-functionalized monomers containing primary amine irrespective of the structure of the azide-functionalized monomer. Polymers of **A** and **B** series showed the same trend of toxicity of the azide-functionalized monomers in the order of **4** > **3** > **1** > **2**. It demonstrated that the ethylene glycol unit in the polymer backbone could greatly reduce polymer toxicity. A significant increase in polymer toxicity could be observed once monomers containing ethylene glycol unit were replaced with monomers containing amine group. These results suggested that the amine density of polymer played a critical role in the polymer toxicity. In **C** series, to our surprise, $\mathbf{C_2}$ appeared to be far more toxic than other polymers. Polymers synthesized using monomers **D** were a little less toxic than polymers synthesized using monomers **C**, which indicated that more methylene moiety in polymer backbone could reduce the amine density of the polymers and thus reduce toxicity.

PEI is generally used as a positive control for nonviral gene transfection in many previous papers;[30] however, its severe toxicity limited its in vivo use.[31] By comparing the toxicity of CPs with PEI, it could be found that the toxicity of CPs was much lower than that of PEI. The 100 μg/mL $\mathbf{B_4}$ and 30 μg/mL PEI showed about the same amine concentration. The toxicity of $\mathbf{B_4}$ was very low in MDA-MB-468 cells with cell viability of 69.12% at 100 μg/mL. In contrast, for cells treated with PEI, no cell was viable at polymer concentration of 20 μg/mL after 24 h incubation. The reduced toxicity of CPs compared with PEI could be attributed to the reduced charge density of polymers by the 1,2,3-triazole-amide moiety in the polymer backbone to distribute the positive charge.[32]

3.3. Apoptosis or Necrosis Observation. Apoptosis and necrosis are two fundamental types of cell death. Apoptosis is an active, genetically regulated disassembly of the cell, and necrosis, unlike apoptosis, is considered to be a passive

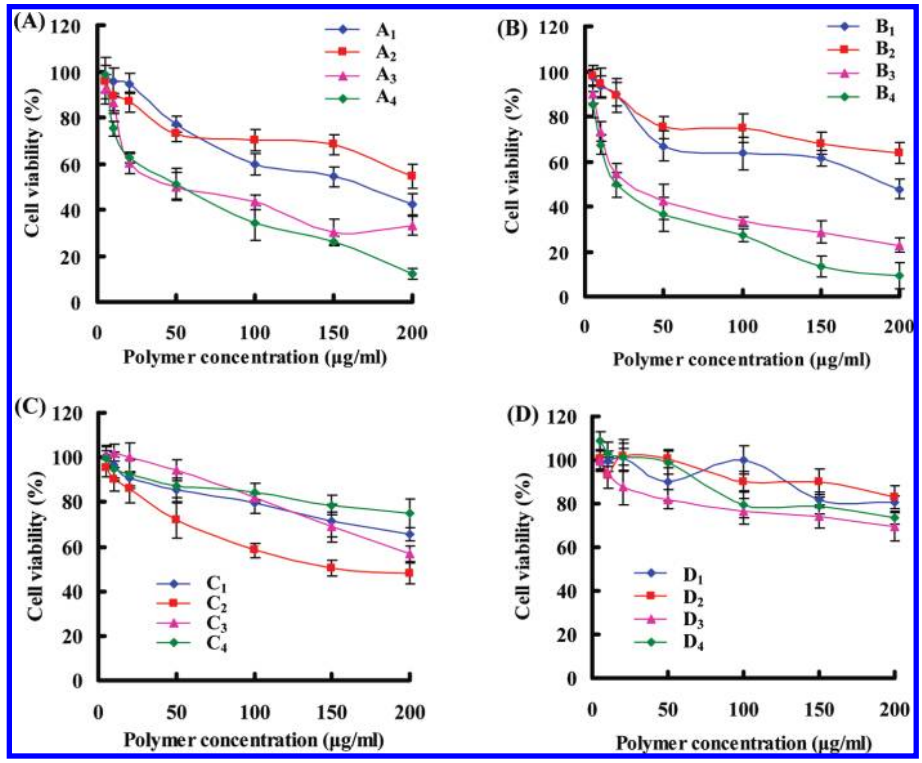

Figure 2. Cytotoxicity of CPs in MDA-MB-468 cells. Cells were incubated with CPs at polymer concentrations ranging from 5 to 200 μg/mL for 24 h. Each data point represents the mean ± SD of six replicates of three times.

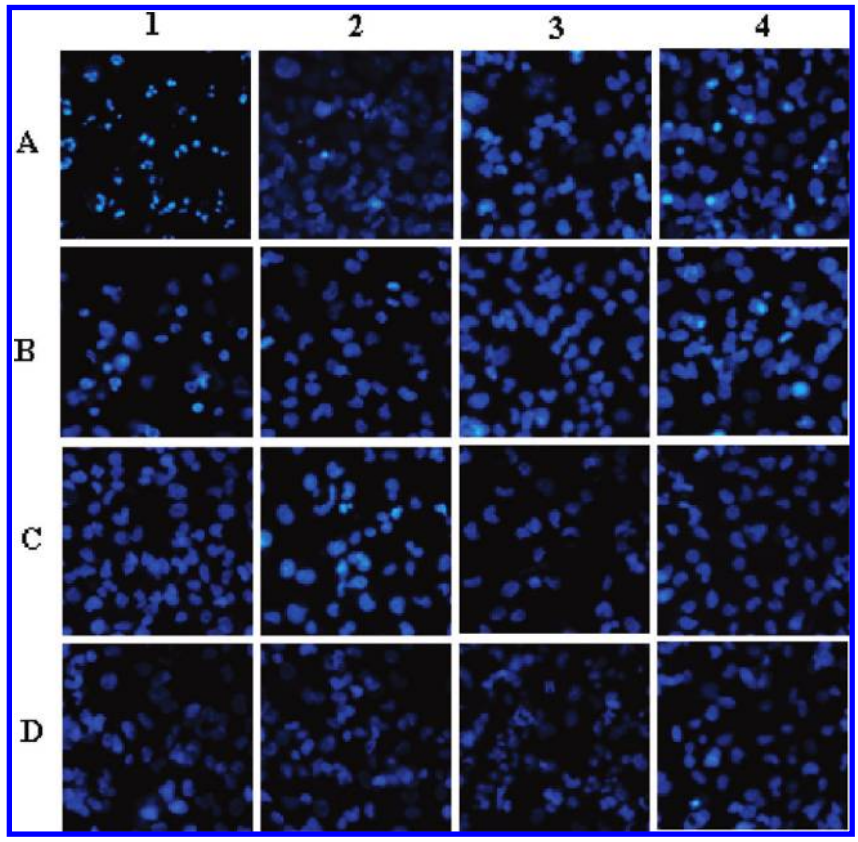

Figure 3. Fluorescence microscopic images of MDA-MB-468 cell nuclei following 24 h of incubation with CPs at polymer concentration of 100 μg/mL. Cell nucleus was stained with Hoechst 33342.

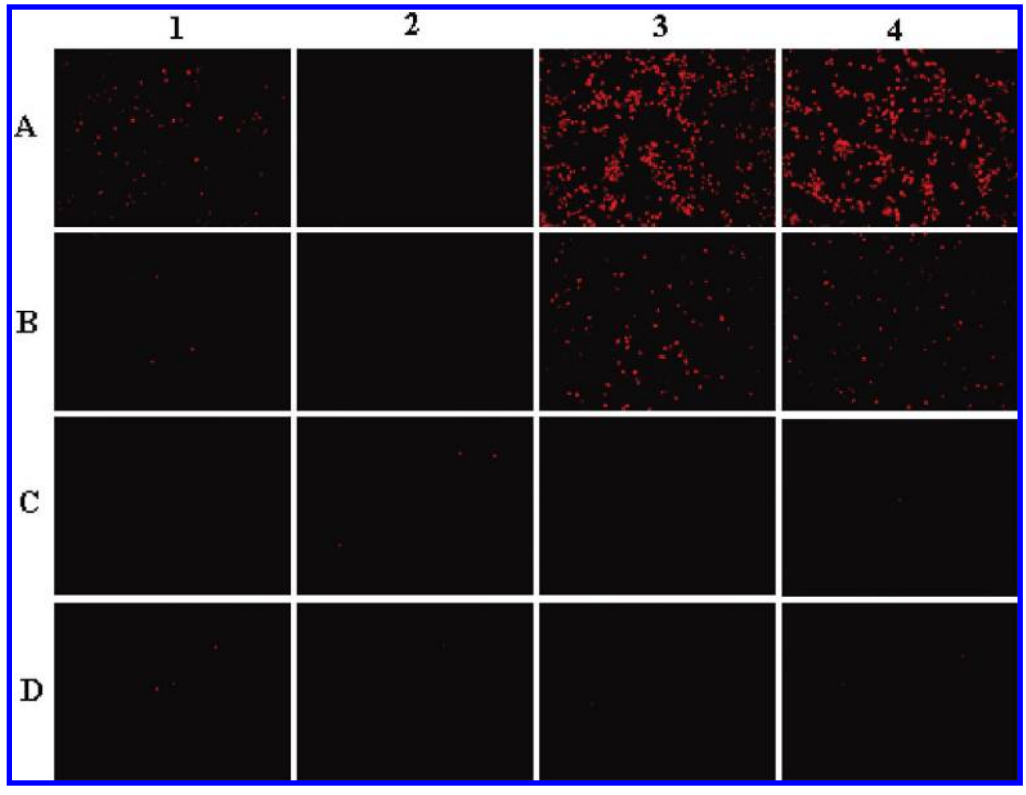

Figure 4. Fluorescence microscopic images of MDA-MB-468 cell nuclei following 24 h of incubation with CPs at polymer concentration of 100 μg/mL. Cell nucleus was stained with PI.

degenerative phenomenon induced by direct toxic and physical injuries.[33,34] A cell undergoing apoptosis demonstrates nuclear condensation and DNA fragmentation, which can be detected by staining with Hoechst 33342 and fluorescence microscopy. PI is not permeant to live cells or apoptotic cells but stains necrotic cells that have lost membrane integrity with red fluorescence. In this work, apoptosis or necrosis was determined by Hoechst 33342 or PI nuclear staining. By this method, it

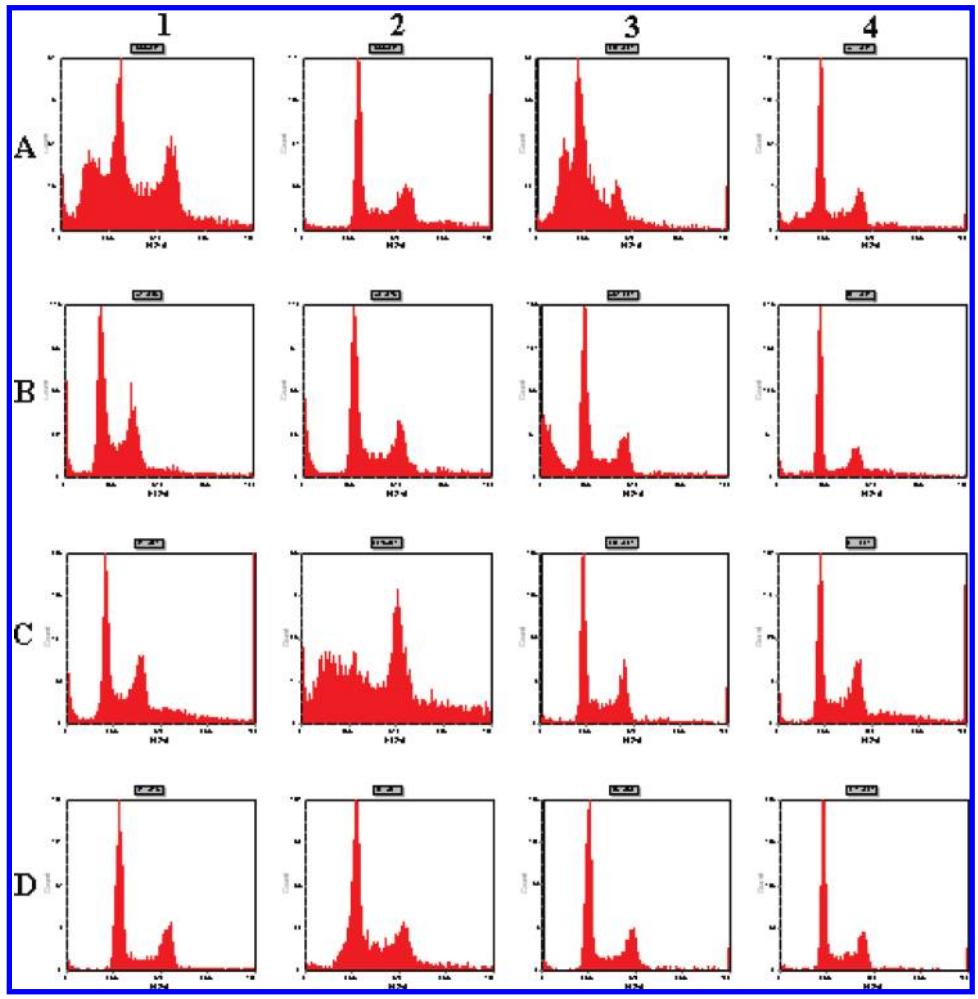

Figure 5. Effects of treatment with CPs at polymer concentration of 100 μg/mL for 24 h on the cell cycle of MDA-MB-468 cells.

was possible to detect, in the same sample and at the same time, intact cells, cells undergoing apoptosis, and dead cells resulting from apoptotic or necrotic processes.

As shown in Figure 3, polymer $\mathbf{A_1}$ at 100 μg/mL could induce severe apoptosis with condensed nuclear chromatin. From Figure 4, the PI staining could be observed in cells treated with polymer $\mathbf{A_1}$, which demonstrated that polymer $\mathbf{A_1}$ could cause cell death through either apoptosis or necrosis. Slight DNA fragmentation was observed in cells treated with $\mathbf{A_3}$. The condensed nuclei characteristic of apoptosis was also observed in cells treated with polymer $\mathbf{B_4}$ or $\mathbf{C_2}$. No induction of necrosis was observed in cells treated with polymer $\mathbf{C_2}$, which indicated that the death of cells treated with polymer $\mathbf{C_2}$ was mainly through apoptosis. From the PI stain study, it could be found that polymer $\mathbf{A_3}$, $\mathbf{A_4}$, $\mathbf{B_3}$, or $\mathbf{B_4}$ caused severe cell necrosis (Figure 4). The high cellular toxicity of $\mathbf{A_3}$, $\mathbf{A_4}$, $\mathbf{B_3}$, or $\mathbf{B_4}$ was consistent with the results of MTT tests. Compared with polymers $\mathbf{A_1}$, $\mathbf{A_2}$, $\mathbf{B_1}$, and $\mathbf{B_2}$, the high toxicity of $\mathbf{A_3}$, $\mathbf{A_4}$, $\mathbf{B_3}$, or $\mathbf{B_4}$ could be attributed to the high amine density of CPs, which could cause more severe cell injury and resultant cell death. Except $\mathbf{C_2}$, polymers of **C** or **D** series did not induce apoptosis or necrosis in MDA-MB-468 cells. These results demonstrated that the toxicity of polymers containing primary amine was much lower than that of polymers containing secondary amine.

3.4. Cell Cycle Analysis. Cell cycle analysis is a sensitive test for the toxicity of test materials to the proliferating cells. Many conventional anticancer drugs such as taxol and anthracyclines act by blocking one or more stages of the cell cycle to inhibit cell proliferation.[35] Many synthetic polymeric materials also demonstrated cell-cycle-dependent toxicity. It was reported that the toxicity of the synthetic peptide seemed to be strongly related to the cell cycle, more precisely to the hyperpolarization occurring at the G1/S transition.[36]

Flow cytometric analysis (FCM) of cell cycle indicated that polymers $\mathbf{A_1}$, $\mathbf{A_3}$, $\mathbf{C_2}$ exerted toxic effect on MDA-MB-468 cells and induced cell apoptosis as highly definable sub-G1 peaks occurred (Figure 5). An increase in G2/M peak could also be observed in cells treated with polymer $\mathbf{C_2}$, which indicated that polymer $\mathbf{C_2}$ could inhibit cell growth by inducing cell cycle arrest and apoptosis. No obvious changes of cell cycle phase were found in all other CPs, which indicated that their cellular toxicity was not related to cell cycle arrest.

3.5. Hemolysis Assay. When cationic polyplexes are administrated intravenously, the interactions between positively

Table 1. Hemolysis Assay of CPs[a]

polymer	hemolysis rate (%)	polymer	hemolysis rate (%)
$\mathbf{A_1}$	2.64 ± 0.58	$\mathbf{C_1}$	0.78 ± 0.11
$\mathbf{A_2}$	0.73 ± 0.10	$\mathbf{C_2}$	1.92 ± 0.37
$\mathbf{A_3}$	2.19 ± 0.30	$\mathbf{C_3}$	2.24 ± 0.09
$\mathbf{A_4}$	3.96 ± 0.30	$\mathbf{C_4}$	2.64 ± 0.21
$\mathbf{B_1}$	0.85 ± 0.15	$\mathbf{D_1}$	2.26 ± 0.09
$\mathbf{B_2}$	0.86 ± 0.05	$\mathbf{D_2}$	2.10 ± 0.08
$\mathbf{B_3}$	3.68 ± 0.63	$\mathbf{D_3}$	1.82 ± 0.19
$\mathbf{B_4}$	3.87 ± 0.78	$\mathbf{D_4}$	1.62 ± 0.18

[a] Erythrocytes were incubated with CPs at polymer concentration 100 μg/mL for 3 h. 0.9% NaCl solution was used as the negative control with 0% hemolysis, and DD H_2O was used as the positive control with 100% hemolysis. All hemolysis data were presented as the percentage of the complete hemolysis. Data were given as mean ± SD (n = 3).

Table 2. Characterization of CPs

polymer	M_w (Da)	M_w/M_n	yield (%)	polymer	M_w (Da)	M_w/M_n	yield (%)
$\mathbf{A_1}$	15 480	1.13	31	$\mathbf{C_1}$	15 640	1.16	43
$\mathbf{A_2}$	17 221	1.15	28	$\mathbf{C_2}$	15 990	1.21	56
$\mathbf{A_3}$	15 557	1.21	25	$\mathbf{C_3}$	15 778	1.15	39
$\mathbf{A_4}$	14 014	1.14	36	$\mathbf{C_4}$	12 857	1.12	47
$\mathbf{B_1}$	16 940	1.14	34	$\mathbf{D_1}$	14 050	1.20	54
$\mathbf{B_2}$	15 166	1.16	38	$\mathbf{D_2}$	12 879	1.11	49
$\mathbf{B_3}$	14 923	1.22	31	$\mathbf{D_3}$	16 207	1.18	41
$\mathbf{B_4}$	15 139	1.12	39	$\mathbf{D_4}$	14 966	1.13	64

charged polymers and negatively charged erythrocytes are inevitable. Therefore, it is very necessary to test the blood compatibility of new gene delivery vectors. Hemolysis was one of the most important phenomena in the determination of the biocompatibility of the synthetic materials.[37] Toxicity of materials to human red blood cells (RBCs) could disturb the erythrocyte membrane and induce hemoglobin release. As shown in Table 1, the hemolysis rates of blood samples treated with 100 μg/mL CPs were all <5%, which was not considered to be hemolytic. These results proved that CPs were not erythrocyte membrane lytic. Among the 16 CPs, the percentage of hemolysis detected with polymer $\mathbf{A_4}$ and $\mathbf{B_4}$ demonstrated >3.8%, which indicated that CPs containing both second amine and ternary amine could interact more strongly with negatively charged erythrocyte membrane than CPs containing other amines.

3.6. Erythrocyte Aggregation Assay. Because cationic polymer could electrostatically interact with anionic cell membrane and elevate the electrostatic repulsion among RBCs, erythrocyte aggregation usually occurs when the cationic gene delivery vectors are administrated intravenously. RBC aggregation not only affects blood viscosity and microvascular flow dynamics but also alters pharmacokinetics, which in turn might affect the tissue distribution of injected delivery vectors.[38] Therefore, RBC aggregation has been considered to be one of the major factors affecting transfection efficiency of gene delivery carriers.

To investigate the interaction of CPs with erythrocytes, the morphology of erythrocytes after treatment with CPs was examined under light microscopy. It could be seen that all CPs could induce erythrocyte aggregation due to their positive charged property (Figure 6). Polymer $\mathbf{B_1}$, $\mathbf{B_2}$, $\mathbf{D_1}$, and $\mathbf{D_2}$ showed relatively low levels of aggregation. Polymer $\mathbf{A_1}$, $\mathbf{A_3}$, $\mathbf{B_3}$, $\mathbf{D_3}$, and $\mathbf{D_4}$ could cause severe erythrocyte aggregation, which indicated that the CPs with higher amine density caused more severe RBC aggregation. In the **B**, **C**, or **D** series, it could be found obviously that the introduction of ethylene glycol group in the polymer backbone could reduce the interaction between polymers and erythrocytes. The interaction reduced as the number of the ethylene glycol group in the polymer backbone increased ($\mathbf{A_2} < \mathbf{A_1}$, $\mathbf{B_2} < \mathbf{B_1}$). No obvious RBC aggregation was observed after treatment with $\mathbf{A_4}$ or $\mathbf{B_4}$, but erythrocyte membrane disturbance was found from the microscopic images. These results demonstrated that $\mathbf{A_4}$ and $\mathbf{B_4}$ showed relatively high hemotoxicity.

3.7. In Vitro Transfection. By summing up all data from the biocompatibility study, polymers $\mathbf{B_1}$ and $\mathbf{B_2}$ showed good biocompatibility, inducing neither apoptosis nor necrosis at the

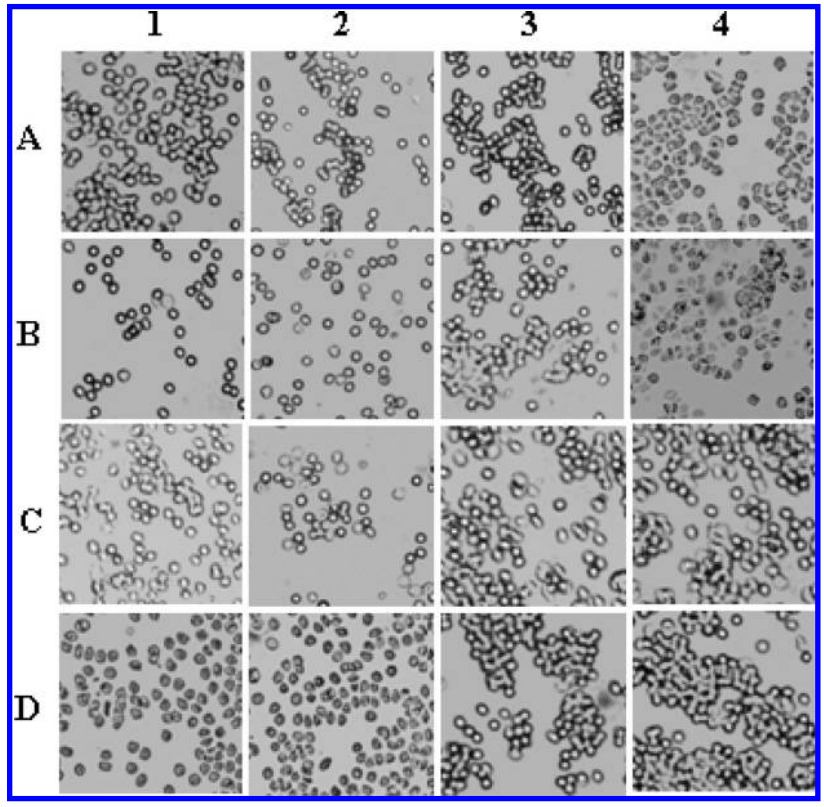

Figure 6. Microscopic images of erythrocytes following incubation with CPs at polymer concentration of 100 μg/mL for 3 h.

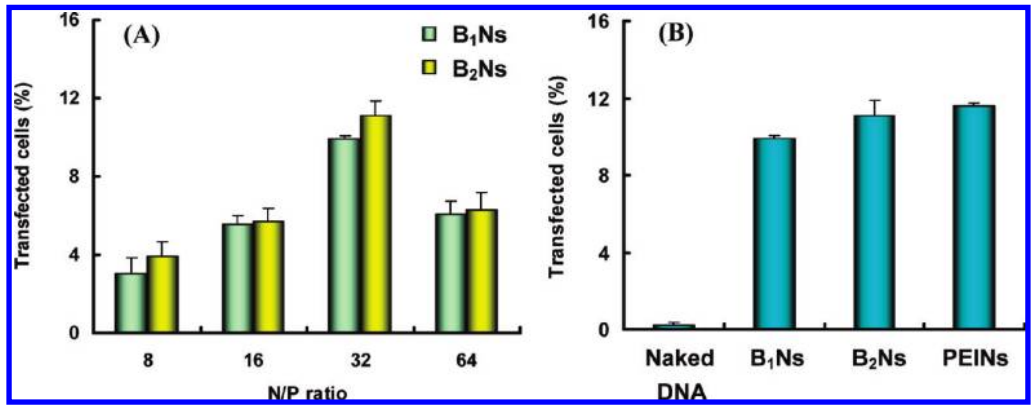

Figure 7. In vitro transfection efficiency of CPNs against MDA-MB-468 cells. (A) Transfection efficiency of **B_1**/DNA complex nanoparticles (**B_1Ns**) and **B_2**/DNA complex nanoparticles (**B_2Ns**) at different N/P ratios. (B) Transfection efficiency of **B_1Ns** and **B_2Ns** at N/P ratio of 32 compared with that of PEINs at mass ratio 3 and naked DNA with plasmid dosage of 2.5 μg/well.

test concentration. They also demonstrated low hemolysis ratio and erythrocyte aggregation. Therefore, we chose **B_1** and **B_2** to investigate preliminarily their transfection ability.

For effective gene delivery, cationic polymer should have the ability to condense DNA into nanoparticles. Both **B_1** and **B_2** could form nanoparticles with DNA in water at N/P ratio ≥ 1. The particle sizes of **B_1**/DNA complex nanoparticles (**B_1Ns**) and **B_2/DNA** complex nanoparticles (**B_2Ns**) decreased with the N/P ratio increasing and decreased to constant value in the range of 160 to 220 nm when the N/P ratios increased from 8 to 64. The particle sizes of **B_1Ns** and **B_2Ns** at N/P ratio of 32 were 171.3 $\pm$ 17.3 and 208.3 $\pm$ 10.0 nm, respectively. The ζ potentials of **B_1Ns** and **B_2Ns** were 20.6 $\pm$ 0.8 and 21.6 $\pm$ 1.0 mV, respectively.

The ability to withstand serum challenge to some extent is a very important property for cationic polymer/DNA complex nanoparticles because the instability of polyplexes in serum could greatly limit their transfection efficiency.[39] It was reported that the presence of serum had great effects on the transfection efficiency of many kinds of polyplexes including PEINs.[39,40] But no obvious effect of serum on the transfection efficiency of **B_1Ns** and **B_2Ns** was found in the transfection experiment, which could attribute to the triazole-amide moiety in the polymer backbone, which served as H-bond acceptors and could increase hydrophobic interactions of the polymer with DNA and thus increase the stability of CPNs in serum.

The influence of N/P ratio on the transfection efficiency of **B_1Ns** and **B_2Ns** was investigated at four N/P ratios (N/P ratio 8, 16, 32, and 64). The highest transfection efficiency was obtained at N/P ratio 32 in MDA-MB-468 cells (Figure 7A). The transfection efficiencies of **B_1Ns** and **B_2Ns** at N/P ratio 32 were compared with naked DNA and PEINs at mass ratio 3. The results showed that **B_1Ns** and **B_2Ns** exhibited significantly higher transfection efficiency than naked DNA and comparable transfection efficiency in comparison with PEINs, which was the most popular positive control in gene delivery (Figure 7B). Compared with PEINs, the improved stability in serum, decreased cytotoxicity, and comparable transfection efficiency made the CPNs formed by novel CPs, promising for safe and efficient gene delivery.

4. Conclusions

In this work, 16 new cationic CPs were parallelly synthesized via the conjugation of four alkyne-functionalized monomers to four azide-functionalized monomers by "click chemistry", and the structure-biocompatibility of CPs was evaluated by in vitro cytotoxicity and blood compatibility tests. In **A** and **B** series, polymers **B_1** and **B_2** showed good biocompatibility, inducing neither apoptosis nor necrosis at the test concentration. They also demonstrated low hemolysis ratio and erythrocyte aggregation. In **C** and **D** series, except **C_2**, the cytotoxicity of all polymers was low, inducing neither apoptosis nor necrosis at the test concentration. All polymers in **C** and **D** series could cause RBC aggregation, except **D_1** and **D_2**. Polymers **B_1** and **B_2** with good biocompatibility exhibited comparable transfection efficiency in comparison with PEI (25 kDa) but much lower cytotoxicity. These results suggested that the new cationic CPs could be promising carriers for gene delivery. Future work will involve in the evaluation of the structure−activity relationship of CPs.

Acknowledgment. The National Basic Research Program of China (2010CB934000 and 2007CB935800), the National Natural Science Foundation of China (30925041 and 30901866), National Science & Technology Major Project "Key New Drug Creation and Manufacturing Program" (No. 2009ZX09501-024 and 2009ZX09301-001), and Shanghai Nanomedicine Program (0852 nm05700) are gratefully acknowledged for financial support.

References and Notes

(1) Halama, A.; Kuliński, M.; Librowski, T.; Lochyński, S. *Pharmacol. Rep.* **2009**, *61*, 993–999.
(2) Park, T. G.; Jeong, J. H.; Kim, S. W. *Adv. Drug Delivery Rev.* **2006**, *58*, 467–486.
(3) Sun, X.; Zhang, N. *Mini-Rev. Med. Chem.* **2010**, *10*, 108–125.
(4) Tros de Ilarduya, C.; Sun, Y.; Düzgüneş, N. *Eur. J. Pharm. Sci.* **2010**, *40*, 159–170.
(5) Hirko, A.; Tang, F.; Hughes, J. A. *Curr. Med. Chem.* **2003**, *10*, 1185–1193.
(6) Lutz, J. F.; Zarafshani, Z. *Adv. Drug Delivery Rev.* **2008**, *60*, 958–970.
(7) van Dijk, M.; Rijkers, D. T.; Liskamp, R. M.; van Nostrum, C. F.; Hennink, W. E. *Bioconjugate Chem.* **2009**, *20*, 2001–2016.
(8) Rengifo, H. R.; Chen, L.; Grigoras, C.; Ju, J.; Koberstein, J. T. *Langmuir.* **2008**, *24*, 7450–7456.
(9) Tosh, D. K.; Yoo, L. S.; Chinn, M.; Hong, K.; Kilbey, S. M.; Barrett, M. O.; Fricks, I. P.; Harden, T. K.; Gao, Z. G.; Jacobson, K. A. *Bioconjugate Chem.* **2010**, *21*, 372–384.
(10) Franc, G.; Kakkar, A. *Chem. Commun. (Cambridge, U.K.).* **2008**, *42*, 5267–5276.
(11) Kar, M.; Vijayakumar, P. S.; Prasad, B. L.; Sen Gupta, S. *Langmuir.* **2010**, *26*, 5772–5781.
(12) Tang, Y.; Jim, C. K.; Liu, Y.; Ye, L.; Qin, A.; Lam, J. W.; Zhao, C.; Tang, B. Z. *ACS Appl. Mater. Interfaces* **2010**, *2*, 566–574.

(13) van Dijk, M.; Nollet, M. L.; Weijers, P.; Dechesne, A. C.; van Nostrum, C. F.; Hennink, W. E.; Rijkers, D. T. S.; Liskamp, R. M. J. *Biomacromolecules* **2008**, *9*, 2834–2843.
(14) Srinivasachari, S.; Liu, Y. M.; Zhang, G. D.; Prevette, L.; Reineke, T. M. *J. Am. Chem. Soc.* **2006**, *128*, 8176–8184.
(15) Srinivasachari, S.; Liu, Y. M.; Prevette, L. E.; Reineke, T. M. *Biomaterials* **2007**, *28*, 2885–2898.
(16) Vogel, B. M.; Cabral, J. T.; Eidelman, N.; Narasimhan, B.; Mallapragada., S. K. *J. Comb. Chem.* **2005**, *7*, 921–928.
(17) Barua, S.; Joshi, A.; Banerjee, A.; Matthews, D.; Sharfstein, S. T.; Cramer, S. M.; Kane, R. S.; Rege, K. *Mol. Pharm.* **2009**, *6*, 86–97.
(18) Akinc, A.; Lynn, D. M.; Anderson, D. G.; Langer, R. *J. Am. Chem. Soc.* **2003**, *125*, 5316–5123.
(19) Anderson, D. G.; Lynn, D. M.; Langer, R. *Angew. Chem., Int. Ed.* **2003**, *42*, 3153–3158.
(20) Cao, D. X.; Qiao, B.; Ge, Z. Q.; Yuan, Y. J. *Cancer Lett.* **2004**, *214*, 103–113.
(21) Lin, C.; Zhong, Z.; Lok, M. C.; Jiang, X.; Hennink, W. E.; Feijen, J.; Engbersen, J. F. J. *J. Controlled Release* **2006**, *116*, 130–137.
(22) Zelikin, A. N.; Putnam, D.; Shastri, P.; Langer, R.; Izumrudov, V. A. *Bioconjugate Chem.* **2002**, *13*, 548–553.
(23) Thomas, M.; Klibanov, A. M. *Proc. Natl. Acad. Sci. U.S.A.* **2002**, *99*, 14640–14645.
(24) Murthy, R.; Shell, C. E.; Grunlan, M. A. *Biomaterials* **2009**, *30*, 2433–2439.
(25) Jin, Z. L.; Feng, W.; Beisser, K.; Zhu, S. P.; Sheardown, H.; Brash, J. L. *Colloids Surf., B* **2009**, *70*, 53–59.
(26) Vogel, B. M.; Mallapragada, S. K. *Biomaterials* **2005**, *26*, 721–728.
(27) Miyata, K.; Oba, M.; Nakanishi, M.; Fukushima, S.; Yamasaki, Y.; Koyama, H.; Nishiyama, N.; Kataoka, K. *J. Am. Chem. Soc.* **2008**, *130*, 16287–16294.
(28) Rostovtsev, V. V.; Green, L. G.; Fokin, V. V.; Sharpless, K. B. *Angew Chem., Int. Ed.* **2002**, *41*, 2596–2599.
(29) Diaz, D. D.; Punna, S.; Holzer, P.; McPherson, A. K.; Sharpless, K. B.; Fokin, V. V.; Finn, M. G. *J. Polym. Sci., Part A: Polym. Chem.* **2004**, *42*, 4392–4403.
(30) van Gaal, E. V.; Oosting, R. S.; Hennink, W. E.; Crommelin, D. J.; Mastrobattista, E. *Int. J. Pharm.* **2010**, *390*, 76–83.
(31) Godbey, W. T.; Wu, K. K.; Mikos, A. G. *Biomaterials* **2001**, *22*, 471–480.
(32) Lv, H.; Zhang, S.; Wang, B.; Cui, S.; Yan, J. *J. Controlled Release* **2006**, *114*, 100–109.
(33) Kanduc, D.; Mittelman, A.; Serpico, R.; Sinigaglia, E.; Sinha, A. A.; Natale, C.; Santacroce, R.; Di Corcia, M. G.; Lucchese, A.; Dini, L.; Pani, P.; Santacroce, S.; Simone, S.; Bucci, R.; Farber, E. *Int. J. Oncol.* **2002**, *21*, 165–170.
(34) Farber, E. *Mod. Pathol.* **1994**, *7*, 605–609.
(35) Das, G. C.; Holiday, D.; Gallardo, R.; Haas, C. *Cancer Lett.* **2001**, *165*, 147–153.
(36) Pellegrin, P.; Menard, C.; Mery, J.; Lory, P.; Charnet, P.; Bennes, R. *FEBS Lett.* **1997**, *418*, 101–105.
(37) Müller, U. *Eur. Med. Device Technol.* **2008**, *19*, 32–34.
(38) Baskurt, O. K.; Meiselman, H. J. *Microcirculation* **2008**, *15*, 585–590.
(39) Christensen, L. V.; Chang, C. W.; Kim, W. J.; Kim, S. W.; Zhong, Z.; Lin, C.; Engbersen, J. F.; Feijen, J. *Bioconjugate Chem.* **2006**, *17*, 1233–1240.
(40) Kim, T. I.; Ou, M.; Lee, M.; Kim, S. W. *Biomaterials* **2009**, *30*, 658–664.

BM100906M